
DYNAMICS CHAOS IN RADIOPHYSICS
AND ELECTRONICS

Specific Features of Generalized Synchronization in Unidirectionally and Mutually Coupled Mappings and Flows: Method of Phase Tubes

A. A. Koronovskii^{a, b}, O. I. Moskalenko^{a, b}, A. E. Khramov^{a, b}, and S. A. Shurygina^a

^aChernyshevskii State University, Astrakhanskaya ul. 83, Saratov, 410012 Russia

^bGagarin State Technical University, Politeknicheskaya ul. 77, Saratov, 410054 Russia

e-mail: moskalenko@nonlin.sgu.ru, shrs@nonlin.sgu.ru

Received January 28, 2013

Abstract—A concept of generalized synchronization in flow systems and discrete mappings is corrected and completed. It is rigorously demonstrated that the state vectors of interacting systems in the course of generalized synchronization must be considered as interrelated with the aid of a functional rather than a functional relation (as it is commonly accepted). An approach based on the analysis of the tubes of trajectories in phase space is proposed to determine the threshold of the generalized synchronization and study such type of synchronous behavior in the systems with discrete and continuous time. We conclude that the concept of weak and strong generalized synchronization must also be reconsidered.

DOI: 10.1134/S1064226914100052

INTRODUCTION

Chaotic synchronization of nonlinear dynamic systems is a universal phenomenon that is important for fundamental and practical applications [1–3]. The synchronization can be observed in radio physical, physical, physiological, biological, chemical, social, and several other systems. Multiple types of the synchronous behavior of chaotic oscillators are being analyzed. The regime of generalized chaotic synchronization (GCS) is one of the most interesting regimes [4].

It is commonly accepted that the regime of generalized synchronization is introduced for a system of two unidirectionally coupled chaotic oscillators or discrete mappings. This means that a functional relation is established between the states of such systems after the transient process [4]. The functional relation can be rather complicated, and a procedure that makes it possible to find such a relation can be nontrivial. Based on the type (smooth or fractal) of the functional relation, strong or weak generalized synchronization can be analyzed [5]. The strong synchronization corresponds to the smooth dependence of the coordinates of the drive and response systems whereas the fractal dependence is observed for the weak synchronization. In the latter case, two different dynamic systems may serve as interacting oscillators (including systems with different dimensions of phase space) and the method of auxiliary system [6] is employed for diagnostics of the synchronous regime.

Note that the determination of the functional relation in the GCS regime can be rigorously demon-

strated for two unidirectionally coupled oscillators with continuous time [7]. In the case of the mutual coupling, the corresponding analysis is inapplicable, the functional dependence of the state vectors of the systems is not proven, and the very existence of such a dependence is questionable. Even a more complicated scenario corresponds to the systems with discrete time. Invertible mappings are related to flow systems with the aid of the Poincaré cross section [8]. Therefore, the proof of existence of the functional relation for state vectors of interacting systems can be extended only to unidirectionally coupled invertible mappings. The existence of such a dependence is questionable for irreversible mappings and mappings with mutual coupling. Nevertheless, the GCS regime is unfoundedly interpreted as the presence of functional relation.

The method of auxiliary system is supplemented with the method of nearest neighbors [4, 9] and the method of calculation of the spectrum of Lyapunov exponents [10] in the diagnostics of the GCS regime. Both methods can be used to analyze the GCS in the systems with mutual coupling [11]. However, the diagnostics of the GCS in such systems with the aid of the method of auxiliary system leads to incorrect results [12].

In this work, we reconsider and specify the existing concept of the GCS. We show that the states of interacting systems in the GCS regime in both flow systems and discrete mappings must be considered as the states that are interrelated using a functional rather than a functional relation.

1. THEORY OF GENERALIZED CHAOTIC SYNCHRONIZATION

To demonstrate that the GCS concept must be reconsidered and specified, we analyze the dynamics of two unidirectionally coupled flow systems and discrete mappings.

The evolution of states of interacting flow systems is determined using the system of equations

$$\begin{aligned} \dot{\vec{x}} &= \mathbf{H}(\vec{x}, \vec{g}_x), \\ \dot{\vec{y}} &= \mathbf{G}(\vec{y}, \vec{g}_y) + \sigma \mathbf{P}(\vec{x}, \vec{y}), \end{aligned} \quad (1)$$

where $\vec{x} = \vec{x}(t)$ and $\vec{y} = \vec{y}(t)$ are state vectors of drive and response systems, respectively; \mathbf{H} and \mathbf{G} are evolution operators that determine the vector fields of the systems under study; \vec{g}_x and \vec{g}_y are vectors of parameters; function \mathbf{P} is responsible for the unidirectional coupling of the systems; and parameter σ characterizes the coupling strength.

For mappings, such evolution of the state vectors of drive \vec{x}_n and response \vec{y}_n systems is represented as

$$\begin{aligned} \vec{x}_{n+1} &= \mathbf{H}(\vec{x}_n, \vec{g}_x), \\ \vec{y}_{n+1} &= \mathbf{G}(\vec{y}_n, \vec{g}_y) + \sigma \mathbf{P}(\vec{x}_n, \vec{y}_n). \end{aligned} \quad (2)$$

Without loss of generality, we assume that interacting systems \vec{x} and \vec{y} have identical dimensions m .

As was mentioned, the GCS regime for the system with unidirectional coupling corresponds to the existence of a functional relation of the states of interacting systems. For unidirectionally coupled flow systems [4, 5], such a relation is given by

$$\vec{y}(t) = \mathbf{F}[\vec{x}(t)]. \quad (3)$$

For discrete mappings, the relation is written as

$$\vec{y}_n = \mathbf{F}[\vec{x}_n]. \quad (4)$$

Based on the existence of the functional relation of interaction systems (expressions (3) and (4)), we conclude that the nearest neighbors in the GCS regime must obey a linearized relationship that can be derived from expression (3) or (4) provided that functional relation $\mathbf{F}[\cdot]$ is continuously differentiable.

We choose an arbitrary reference point \vec{x}_0 in the drive system ($(\vec{x}_0 = \vec{x}(t_0)$ for flows and $\vec{x}_0 = \vec{x}_N$ for mappings). Point $\vec{y}_0 = \vec{y}(t_0)$ [$\vec{y}_0 = \vec{y}_N$] in the response system corresponds to this point.¹ Let $\vec{x}_j = \vec{x}(t_j)$ [$\vec{x}_j = \vec{x}_{n_j}$] be a point in the drive system that is close to reference point \vec{x}_0 such that $|\vec{x}_j - \vec{x}_0| < \varepsilon$. Then, $\vec{y}_j = \vec{y}(t_j)$ [$\vec{y}_j = \vec{y}_{n_j}$] is the corresponding point in the response system. Vectors of deviation of a phase point from reference point \vec{x}_0 in the drive system and reference point \vec{y}_0 in the response system are written as

$\delta\vec{x}_j = \vec{x}_j - \vec{x}_0$ and $\delta\vec{y}_j = \vec{y}_j - \vec{y}_0$, respectively. With allowance for expressions (3) and (4), we obtain the following formulas for the GCS regime:

$$\begin{aligned} \vec{y}_j &= \vec{y}_0 + \delta\vec{y}_j = \mathbf{F}[\vec{x}_j] \\ &= \mathbf{F}[\vec{x}_0 + \delta\vec{x}_j] \approx \mathbf{F}[\vec{x}_0] + \mathbf{JF}[\vec{x}_0]\delta\vec{x}_j. \end{aligned} \quad (5)$$

Here, $\mathbf{JF}[\vec{x}_0]$ is the Jacobian of $\mathbf{F}[\cdot]$ that is calculated at point \vec{x}_0 . For a finite-dimensional dynamic system with dimension of phase space m , the Jacobian is an m -dimensional square matrix.

In the GCS regime, the following relationship is valid:

$$\vec{y}_0 = \mathbf{F}[\vec{x}_0]. \quad (6)$$

Hence, expression (5) can be represented as

$$\delta\vec{y}_j = \mathbf{A}\delta\vec{x}_j, \quad (7)$$

where $\mathbf{A} = \mathbf{JF}[\vec{x}_0]$ is an $m \times m$ square matrix. If a functional relation of the state vector exists, a similar expression can be derived for mutually coupled chaotic oscillators. In this case, functional relation (3) can be represented as $\mathbf{F}[\vec{x}(t), \vec{y}(t)] = 0$ and relation (4) can be represented as $\mathbf{F}[\vec{x}_n, \vec{y}_n] = 0$.

Thus, the above analysis shows that relationship (7) is valid for two chaotic oscillators or discrete mappings in the GCS regime if the differentiable functional relation exists. Evidently, different matrices $\mathbf{A} = \{a_{ij}\}$ correspond to different reference points \vec{x}_0 and the explicit representation of matrix coefficients a_{ij} is unknown. However, the validity of expression (7) can be verified for two interacting systems with dimension of phase space m if $M > m$ nearest neighbors \vec{x}_j of a fixed reference point \vec{x}_0 and the corresponding vectors \vec{y}_0 and \vec{y}_j are known.

Based on the preliminary analysis of the GCS regime using the method of auxiliary system [6] or calculations of the Lyapunov exponents [10], we can choose m nearest neighbors (from M existing neighbors) and expression (7) must be valid for each J th state \vec{x}_j, \vec{y}_j . In other words, m states yield m^2 linear equations with m^2 unknown quantities (coefficients a_{ij} of matrix \mathbf{A}). Then, the solution to this system of linear equations makes it possible to determine coefficients a_{ij} of matrix \mathbf{A} and the remaining $(M - m)$ states can be used to verify expression (7).

Obviously, a unique solution to the above system of linear equations always exists provided that m states \vec{x}_j that are used for its construction are not linearly dependent. For a relatively large set of states (M is significantly greater than m), m linearly independent reference states can easily be selected. To minimize the error, we must choose such vectors \vec{x}_j and $\delta\vec{x}_j$ for which $|\det(\delta\mathbf{X})| = \max$, where $\delta\mathbf{X}$ is the matrix that

¹ Due to the fact that flow systems and discrete mappings are interrelated, we consider only flow systems and present analogous quantities and relationships for discrete mappings in square brackets.

consists of components of vectors $\delta\bar{x}_j$ corresponding to the states of drive system:

$$\delta\mathbf{X} = \begin{pmatrix} \delta x_1^1 & \delta x_2^1 & \dots & \delta x_k^1 & \dots & \delta x_m^1 \\ \delta x_1^2 & \delta x_2^2 & \dots & \delta x_k^2 & \dots & \delta x_m^2 \\ \vdots & \vdots & \ddots & \vdots & \ddots & \vdots \\ \delta x_1^J & \delta x_2^J & \dots & \delta x_k^J & \dots & \delta x_m^J \\ \vdots & \vdots & \ddots & \vdots & \ddots & \vdots \\ \delta x_1^m & \delta x_2^m & \dots & \delta x_k^m & \dots & \delta x_m^m \end{pmatrix}. \quad (8)$$

When relatively long time samples are available, coefficients a_{ij} of matrix \mathbf{A} can always be determined and, hence, the correctness of expression (7) can always be verified. For this purpose, we must calculate vectors

$$\delta\bar{z}_J = \mathbf{A}\delta\bar{x}_J, \quad (9)$$

where $J = M - m, \dots, M$ and compare them with vectors $\delta\bar{y}_J$ that are obtained from the time sample.

2. CORRECTION OF THE GCS DEFINITION

The previous section shows that state vectors of interacting systems in the GCS regime must satisfy expression (7) in the presence of the differentiable functional relation. Expression (7) can be verified using the calculation of perturbation vectors $\delta\bar{z}_J$ (expression (9)) and comparison of the calculated results with vectors $\delta\bar{y}_J$.² However, the calculations of particular systems show that the state vectors of interacting systems do not coincide with the theoretically calculated vectors and the corresponding difference is relatively large. Such results indicate that expression (9) is not satisfied for chaotic oscillators in the general synchronization regime and, hence, expressions (3) and (4) are also not satisfied or $\mathbf{F}[\cdot]$ is not a differentiable functional relation.

Thus, the commonly accepted interpretation of the GCS regime is not valid (or, at least, valid not always and inconvenient) and, consequently, the definition of the GCS regime must be reconsidered and specified. Note also that the specific feature of the method of nearest neighbors that lies in the fact that the method does not allow exact determination of the threshold of the GCS regime (as distinct from the method of auxiliary system and calculation of the largest conditional Lyapunov exponent) is also related to the possible invalidity of relationships (3) and (4).

However, a notion of GCS is not erroneous, since a consistent theory of this phenomenon has been developed in many works. In particular, the synchronism of coupled chaotic oscillators is proven with the aid of the

concept of synchronization of time scales [13, 14] and easily demonstrated using the method of auxiliary system [6] and calculation of the Lyapunov exponent [10]; the effect is interpreted using the method of modified system [15, 16]; etc. In addition, the commonly accepted definition of the GCS effect (expressions (3) and (4)) is valid in several cases (see below). Thus, we need an additional analysis and correction rather than drastic modification of the GCS definition.

The correction of the GCS definition lies in the fact that state $\bar{y}(t)$ of the response system at moment t (state \bar{y}_n at moment of discrete time n for mapping) is determined by both state of drive system $\bar{x}(t)$ [\bar{x}_n] at the same moment and the prehistory of this state over time interval τ (or discrete length of prehistory K). In other words, $\mathbf{F}[\cdot]$ in expressions (3) and (4) must be considered as a functional for flow systems and a quantity that depends on K previous states for discrete mapping rather than a functional dependence.

In accordance with the GCS concept, drive system $\bar{x}(t)$ [\bar{x}_n] affects response system $\bar{y}(t)$ [\bar{y}_n] in the synchronous regime, so that the state of the latter is determined by the drive system. The convergence process is determined by the largest conditional Lyapunov exponent $\lambda_r^1 < 0$. Over time interval τ [K], the drive system induces the transition of the response system to the state that does not depend on the initial conditions (the application of the method of auxiliary system is based on this effect). For different image points in the response and auxiliary systems, the distance between the points decreases with time:

$$l(t) \cong l(0)\exp(\lambda_r^1 t), \quad [l_{n+1} \cong l_0 \exp(\lambda_r^1 n)]. \quad (10)$$

Thus, the state of the response system at moment t [n] depends on the prehistory of the response system over time interval whose duration is proportional to the largest conditional Lyapunov index:

$$\tau \sim 1/|\lambda_r^1| \quad [K \sim 1/|\lambda_r^1|]. \quad (11)$$

Evidently, expression (5), which is derived under assumption that $\mathbf{F}[\cdot]$ is a differentiable function, is not satisfied in this case. Thus, for the flow systems, we have

$$\bar{y}(t) = \mathbf{F}[\bar{x}(s)], \quad t - \tau < s \leq t; \quad (12)$$

and a similar expression for discrete mappings is written as

$$\bar{y}_n = \mathbf{F}[\bar{x}_n, \bar{x}_{n-1}, \dots, \bar{x}_{n-K}]. \quad (13)$$

We consider small deviations $\delta\bar{x}(s)$ [$\delta\bar{x}_k$] and $\delta\bar{y}(s)$ [$\delta\bar{y}_k$] that remain small at time interval $t_0 - \tau \leq s \leq t_0$

² Evidently, we can directly compare state vectors $\bar{y}_0 + \delta\bar{z}_J$ and $\bar{y}_0 + \delta\bar{y}_J$ rather than perturbation vectors $\delta\bar{z}_J$ and $\delta\bar{y}_J$.

$[N - K \leq k \leq N]$. With allowance for the aforesaid facts, expression (7) for flow systems is represented as

$$\delta\bar{y}(t_0) = \int_{t_0-\tau}^{t_0} \mathbf{J}\mathbf{F}[\bar{x}(s)]\delta\bar{x}(s)ds. \quad (14)$$

For discrete mappings, we have

$$\delta\bar{y}_N = \sum_{k=N-K}^N J_{\bar{x}_k} \mathbf{F}[\bar{x}_{N-K}, \dots, \bar{x}_N] \delta\bar{x}_k, \quad (15)$$

where $J_{\bar{x}_k}$ is the Jacobian of the transformation for variable \bar{x}_k ($k = N - K, \dots, N$). Using to the smallness of deviations $\delta\bar{x}(s)$ [$\delta\bar{x}_k$] from reference trajectory $\bar{x}(s)$ [\bar{x}_k], we derive the following expression in the framework of the linear approximation:

$$\delta\bar{x}(s) = \mathbf{B}(s)\delta\bar{x}(t_0), \quad t_0 - \tau < s \leq t_0 \quad (16)$$

where $\mathbf{B}(s)$ is unknown matrix with time-dependent coefficients ($\mathbf{B}(t_0) = \mathbf{E}$), so that we have

$$\delta\bar{x}_k = \mathbf{B}_k \delta\bar{x}_N \quad (17)$$

where \mathbf{B}_k is unknown matrix that is similar to matrix $\mathbf{B}(s)$ for flow systems.³ For the flow systems, we have

$$\delta\bar{y}(t_0) = \int_{t_0-\tau}^{t_0} \mathbf{J}\mathbf{F}[\bar{x}(s)]\mathbf{B}(s)\delta\bar{x}(t_0)ds. \quad (18)$$

For the discrete mappings, we have

$$\delta\bar{y}_N = \sum_{k=N-K}^N J_{\bar{x}_k} \mathbf{F}[\bar{x}_{N-K}, \dots, \bar{x}_N] \mathbf{B}_k \delta\bar{x}_N. \quad (19)$$

Consequently, the expression for the flow systems is represented as

$$\delta\bar{y}(t_0) = \mathbf{C}(t_0)\delta\bar{x}(t_0), \quad (20)$$

where $\mathbf{C}(t_0)$ is a square ($m \times m$) matrix given by

$$\mathbf{C}(t_0) = \int_{t_0-\tau}^{t_0} \mathbf{J}\mathbf{F}[\bar{x}(s)]\mathbf{B}(s)ds. \quad (21)$$

For the discrete mappings, we obtain

$$\delta\bar{y}_N = \mathbf{C}_N \delta\bar{x}_N, \quad (22)$$

where \mathbf{C}_N is a similar matrix ($m \times m$) represented as

$$\mathbf{C}_N = \sum_{k=N-K}^N J_{\bar{x}_k} \mathbf{F}[\bar{x}_{N-K}, \dots, \bar{x}_N] \mathbf{B}_k. \quad (23)$$

It is seen that expressions (20) and (22) are similar. In addition, both expressions formally coincide with expression (7) accurate to notation $\delta\bar{y}_J = \delta\bar{y}(t_0)$, $\mathbf{A} = \mathbf{C}(t_0)$, and $\delta\bar{x}_J = \delta\bar{x}(t_0)$ for flow systems and

³ Except for $\mathbf{B}_N = \mathbf{E}$, where \mathbf{E} is unit matrix.

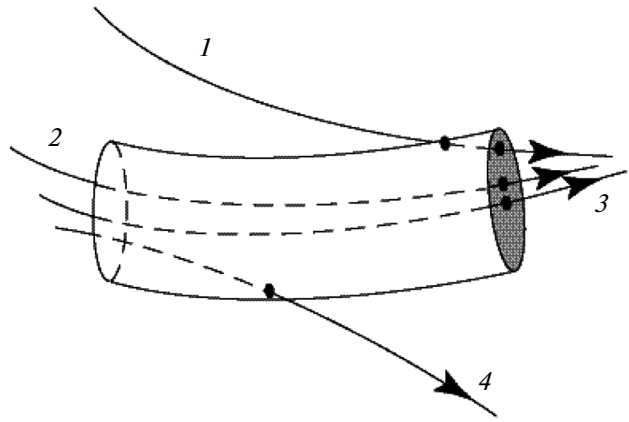


Fig. 1. Phase tube and phase trajectories of the drive system. Reference trajectories 3 and 1 are close to each other at given moment t (shown in gray) but have different prehistories. Trajectories 2 and 3 satisfy the closeness condition and have similar prehistories. Trajectory 4 is not close to trajectories 1–3 at moment t .

$\delta\bar{y}_J = \delta\bar{y}_N$, $\mathbf{A} = \mathbf{C}_N$, and $\delta\bar{x}_J = \delta\bar{x}_N$ for mappings. This circumstance, makes it possible to analyze the development of the generalized synchronization using the calculation of perturbation vectors $\delta\bar{z}_J = \mathbf{C}\delta\bar{x}_J$ (see Section 1) and comparison with vectors $\delta\bar{y}_J$. However, expression (7) is derived under the assumption of closeness of vectors \bar{x}_0 and \bar{x}_J whereas expressions (20) and (22) are obtained under more rigorous conditions for the smallness of the deviations of the phase trajectories at time interval $t_0 - \tau < s < t_0$ [$k = N - K, \dots, N$].

To quantitatively characterize the closeness of the vectors to each other for each pair of vectors $\delta\bar{y}_J$ and $\delta\bar{z}_J$, we consider quantity

$$\Delta_J = \|\delta\bar{y}_J - \delta\bar{z}_J\| / \|\delta\bar{y}_J\| \quad (24)$$

and analyze its distribution.

For chaotic oscillations, phase trajectories in phase space converge along certain directions and diverge along different directions. Therefore, two points that are close to each other in the phase space may have substantially different prehistories if the corresponding phase trajectories in the phase space of the response system are different. Figure 1 illustrates such a scenario. It is seen that the points that correspond to trajectories 3 and 1 are close to each other but the prehistories are different, the condition for smallness of deviation $\delta\bar{x}_J$ at time interval τ (discrete length of prehistory K) is not satisfied, and, hence, expressions (20) and (22) are inapplicable for these points. At the same time, trajectories 2 and 3 satisfy the closeness condition and we may assume that expressions (20) and (22) are satisfied.

To characterize the closeness of the phase trajectories, we use a notion of phase tube. With allowance for the aforesaid facts, the expression that describes the phase tube for the flow systems is written as

$$T_\tau = \{\bar{x} : |\bar{x}_0(s) - \bar{x}| < \varepsilon, \quad s \in [t_0 - \tau; t_0]\} \quad (25)$$

where ε is a small quantity. For the discrete mappings, we have

$$T_K = \{\bar{x} : |\bar{x}_k - \bar{x}| < \varepsilon, \quad k = N - K, \dots, N\}. \quad (26)$$

Both expressions, take into account vectors whose phase trajectories pass through the tube (e.g., trajectory 2 in Fig. 1). Thus, the vectors whose phase trajectories pass through the tube with length τ [K] must be taken into account in the analysis of the GCS regime in the system under study.

3. METHOD OF PHASE TUBES IN THE ANALYSIS OF THE SYSTEMS IN THE GENERALIZED SYNCHRONIZATION REGIME

To verify the correctness of the above analysis, we study specific unidirectionally and mutually coupled dynamic systems (with continuous and discrete time) using the method of phase tubes. First, we consider flow dynamic systems.

3.1. Flow Systems

In the *first example*, we consider two unidirectionally coupled Rössler oscillators:

$$\begin{aligned} \dot{x}_d &= -\omega_d y_d - z_d, & \dot{x}_r &= -\omega_r y_r - z_r + \sigma(x_d - x_r), \\ \dot{y}_d &= \omega_d x_d + a y_d, & \dot{y}_r &= \omega_r x_r + a y_r, \\ \dot{z}_d &= p + z_d(x_d - c), & \dot{z}_r &= p + z_r(x_r - c), \end{aligned} \quad (27)$$

where $\bar{x} = (x_d, y_d, z_d)^T$ [$\bar{y} = (x_r, y_r, z_r)^T$] are the Cartesian coordinates of the drive [response] oscillator; $a = 0.15$, $p = 0.2$, $c = 10.0$, $\omega_r = 0.95$, and $\omega_d = 0.99$ are control parameters that are similar to the parameters of [15, 17]; and σ is the coupling parameter. For such control parameters, the generalized synchronization regime that is determined using the method of auxiliary function and calculation of the Lyapunov exponent is reached at $\sigma_{GS} \approx 0.11$.

We use coupling parameter $\sigma = 0.3$ at which the generalized synchronization regime is reached but the synchronization with delay is not observed and study system (27) using the method of phase tubes (Fig. 2). We consider histograms of the distributions of the normalized difference between vectors $\delta\bar{y}_j$ and $\delta\bar{z}_j$ (24) (Figs. 2a and 2c) and vectors \bar{y}_j and \bar{z}_j (Figs. 2b and 2d) for the scenarios in which all of nearest neighbors (Figs. 2a and 2b) and only points that pass through the phase tube with length $\tau = 100$ (Figs. 2c and 2d) are used (in both cases, we have $\varepsilon = 0.5$). It is seen that significantly different histograms are obtained. The his-

togram represents a δ function for the points that pass through the tube whereas an almost Gaussian distribution is obtained for the scenario in which all of nearest neighbors are used. In the latter case, perturbation vectors \bar{z}_j and \bar{y}_j substantially differ from each other (Fig. 2b). For the points that pass through the tube, calculated perturbation vectors \bar{z}_j are in good agreement with vectors \bar{y}_j , which is in agreement with condition (20) and the assumption that the prehistory must be taken into account. In particular, this means that $\mathbf{F}[\cdot]$ must be considered as a functional for the flow systems.

When the coupling strength of the interacting oscillators increases, the absolute value of the largest conditional Lyapunov exponent $|\lambda_1^r|$ increases and time interval τ (length of the phase tube $T_\tau(t_0)$) decreases, so that quantity τ tends to zero in the vicinity of the threshold of the total synchronization. Therefore, all of neighboring vectors x_j satisfy Eq. (7) in the absence of additional conditions for closeness of phase trajectories in the regime of total synchronization. Thus, the vectors of states of chaotic systems in the GCS regime are related to each other as a functional whereas a functional relation is satisfied for these vectors in the regime of total synchronization.

In the *second example*, we consider a system of two mutually coupled oscillators based on a tunnel diode [18, 19]. The dimensionless system of equations is written as

$$\begin{aligned} \dot{x}_{1,2} &= \omega_{1,2}^2 [h(x_{1,2} - \sigma(y_{2,1} - y_{1,2})) + y_{1,2} - z_{1,2}], \\ \dot{y}_{1,2} &= -x_{1,2} + \sigma(y_{2,1} - y_{1,2}), \\ \mu \dot{z}_{1,2} &= x_{1,2} - f(z_{1,2}), \end{aligned} \quad (28)$$

where $f(\xi) = -\xi + 0.002\text{sh}(5\xi - 7.5) + 2.9$ is the dimensionless characteristic of the nonlinear element; $h = 0.2$, $\mu = 0.1$, $\omega_1 = 1.09$, and $\omega_2 = 1.02$ are the control parameters; and σ is the coupling parameter. Subscripts 1 and 2 correspond to the first and second coupled oscillators. For such control parameters, the regime of generalized synchronization that is determined using the moment at which the second largest Lyapunov exponent becomes negative [11, 12] is reached at $\sigma_{GS} \approx 0.08$.

By analogy with the above analysis of the Rössler systems, we fix the coupling parameter ($\sigma = 0.15$) and study the behavior of system (28) using the method of phase tubes. Figure 3 also presents the histograms of the normalized difference between vectors \bar{z}_j and \bar{y}_j (Figs. 3a and 3c) and vectors (Figs. 3b and 3d) for the parameter that characterizes the phase tube $\varepsilon = 0.5$. Figures 3a and 3b correspond to the scenario in which all of nearest neighbors are used, and Figs. 3c and 3d show the vectors whose phase trajectories pass through the phase tube with length $\tau = 110$. It is seen that vectors \bar{z}_j and \bar{y}_j substantially differ from each other in the first case and the distribution of the normalized

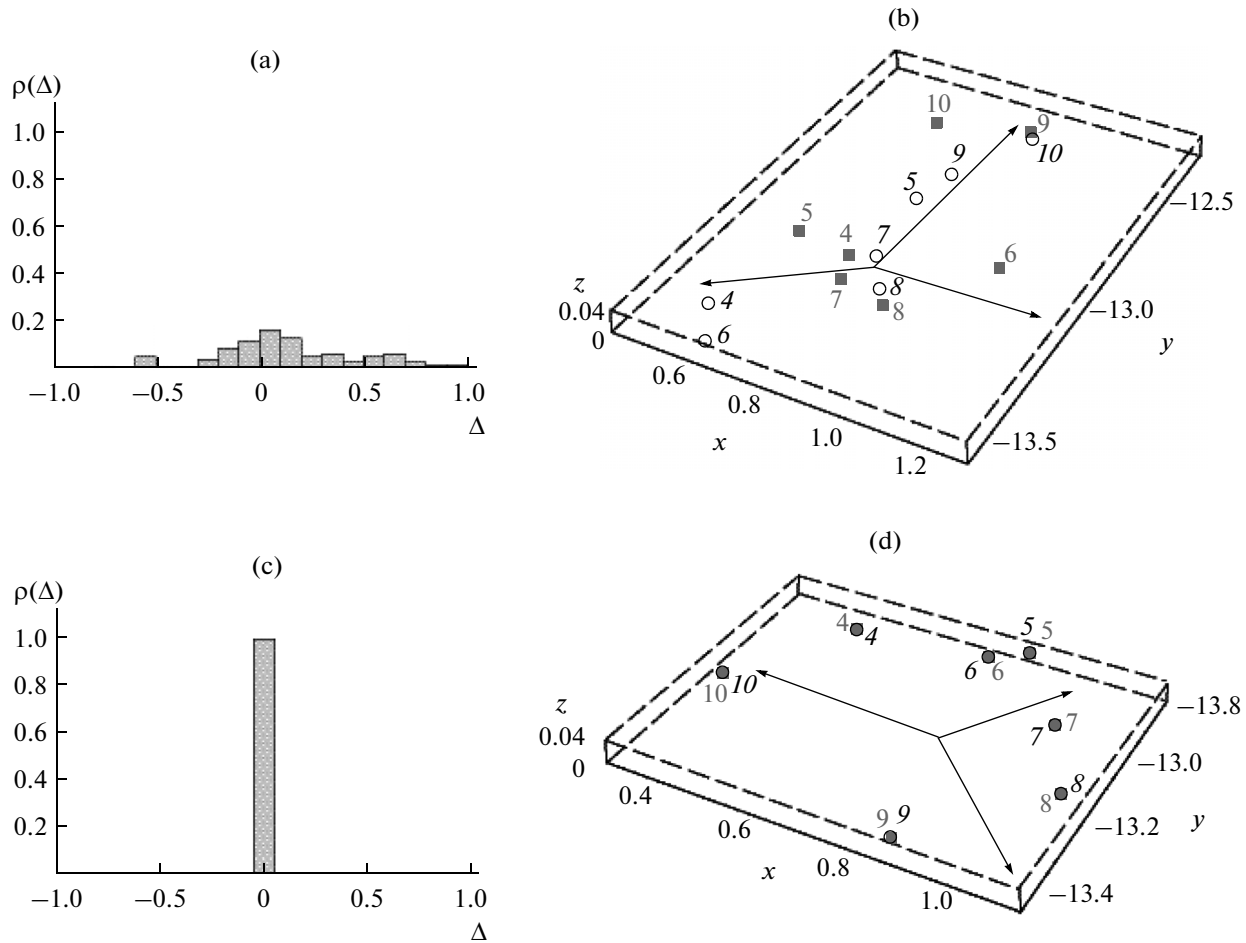


Fig. 2. (a) and (c) Histograms of normalized difference (24) and (b) and (d) corresponding vectors (closed squares 4–10) \bar{y}_j and (open circles 4–10) \bar{z}_j that are calculated for Rössler system (27) at $\sigma = 0.3$ with allowance for (a) and (b) all of nearest neighbors and (c) and (d) points having passed through the tube with length $\tau = 100$.

differences is close to the uniform distribution. In the second case, perturbation vectors \bar{z}_j almost coincide with vectors of the second system \bar{y}_j and the histogram represents a δ function. The results are in good agreement with the results for unidirectionally coupled Rössler oscillators. Therefore, the state vectors of interacting objects in the mutually coupled flow systems are related to each other as a functional (as in the systems with unidirectional coupling).

3.2. Systems with Discrete Time

In the *first example*, we consider two unidirectionally coupled logistic mappings

$$\begin{aligned} x_{n+1} &= f(x_n, a_x), \\ y_{n+1} &= f(y_n, a_y) + \sigma(f(x_n, a_x) - f(y_n, a_y)), \end{aligned} \quad (29)$$

where $f(x, a) = ax(1 - x)$, $a_x = 3.75$ and $a_y = 3.79$ are the control parameters of the drive and response systems, respectively; and σ is the coupling parameter

[5, 20]. With regard to the 1D character of the mappings under study, the vectors from Section 2 must be changed by scalars. Then, the theoretical and analytical regularities remain valid.

The threshold of the GCS regime is determined using the calculation of the conditional Lyapunov exponent for system (29) and specified with the aid of the method of auxiliary system [6]. Figure 4a shows the dependence of conditional Lyapunov exponent λ on coupling parameter σ . It is seen that the conditional Lyapunov exponent is negative for $\sigma \in [0.12; 0.18]$ and $\sigma \geq 0.265$, so that the GCS regime is observed in these intervals. Note that the GCS is close to the total (strong) synchronization at relatively large parameter $\sigma \geq 0.265$ whereas the regime that is classified as the weak GCS corresponds to $\sigma \in [0.12; 0.18]$. Evidently, the prehistory needs not to be taken into account in the regime of strong synchronization, since the states of interacting systems satisfy simple functional relation $y_n \approx x_n$ [5].

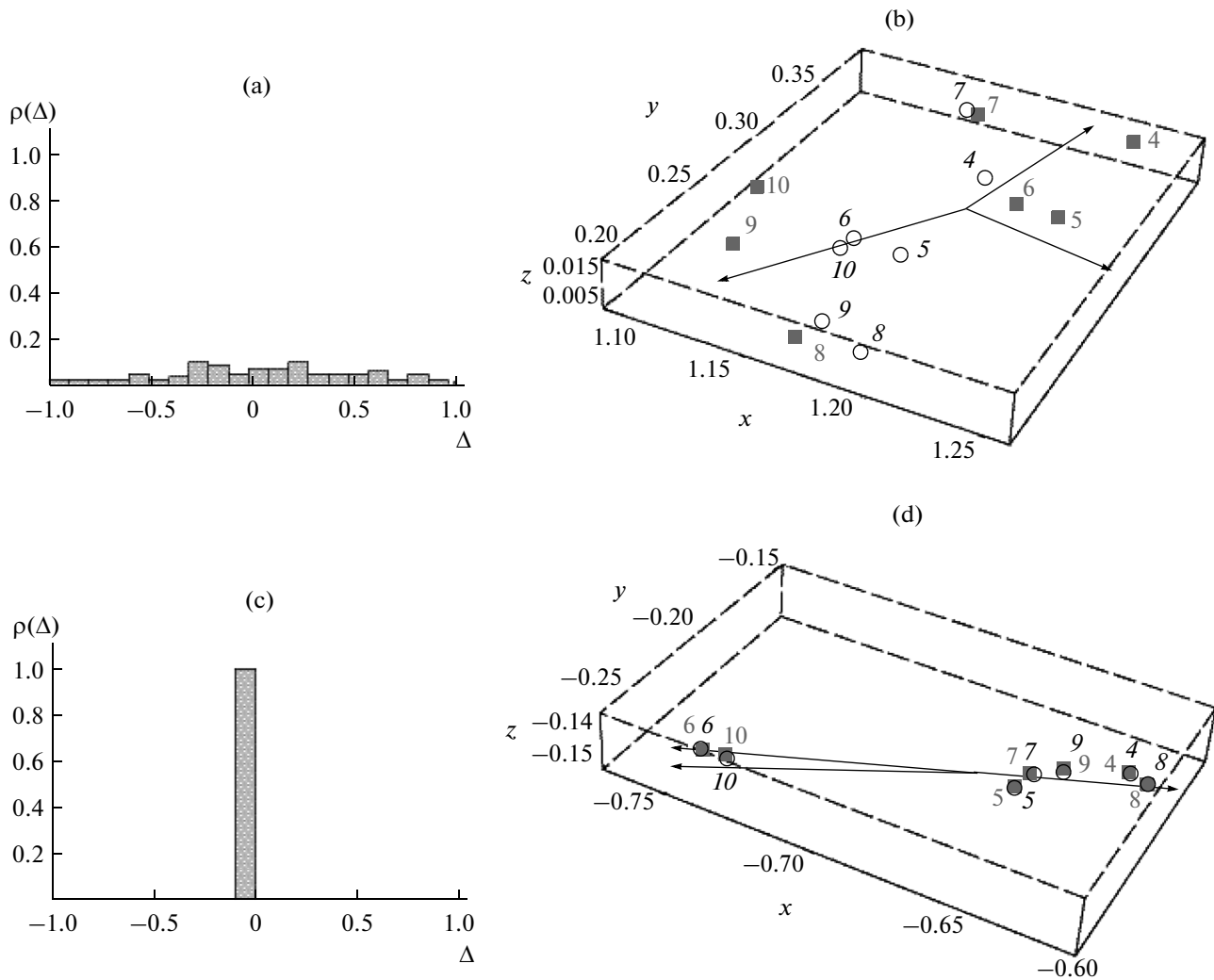


Fig. 3. (a) and (c) Histograms of normalized difference (24) and (b) and (d) corresponding vectors (closed squares 4–10) \bar{y}_J and (open circles 4–10) \bar{z}_J that are calculated for oscillators based on tunnel diode (28) at $\sigma = 0.15$ with allowance for (a) and (b) all of nearest neighbors and (c) and (d) points having passed through the tube with length $\tau = 110$.

However, an additional analysis is needed for the weak synchronization at $\sigma \in [0.12; 0.18]$.

Without loss of generality, we choose coupling parameter $\sigma = 0.14$, which corresponds to the minimum negative conditional Lyapunov exponent (the arrow in Fig. 4a). For accuracy $\varepsilon = 0.01$ in expression (26), we analyze the effect of prehistory length K on quantity δz_J and distribution of normalized difference (24). In this case, we randomly choose reference point x_N . When expression (22) is satisfied, the distribution of normalized differences Δ_J represents a δ function as in the case of flow systems.

Figures 4b, 4d, and 4f present the histograms of normalized differences Δ_J for different prehistory lengths K . Figures 4c, 4e, and 4g show planes (x, y) that characterize the states of drive and response systems for the above values of the control parameters. It

is seen that the dependence of the coordinates of the reference system on the coordinates of the drive system exhibits fractal (nonsmooth) character, which proves the assumption on the weakness of the GCS regime. In each figure, we also present points (x_J, y_J) that satisfy condition (26) for the given prehistory length. Figures 4b and 4c illustrate the scenario in which all of nearest neighbors are taken into account (the prehistory is disregarded and $K = 0$). The scenario corresponds to the conventional concept of the GCS. In this case, normalized difference Δ_J is almost uniformly distributed over interval $[0; 1]$ (Fig. 4b) and the points in the phase space of the response system are also randomly distributed in a wide range of variable y (Fig. 4c). The results show that Eq. (9) is not satisfied in this case.

An increase in the prehistory length leads to the transformation of the distribution of normalized dif-

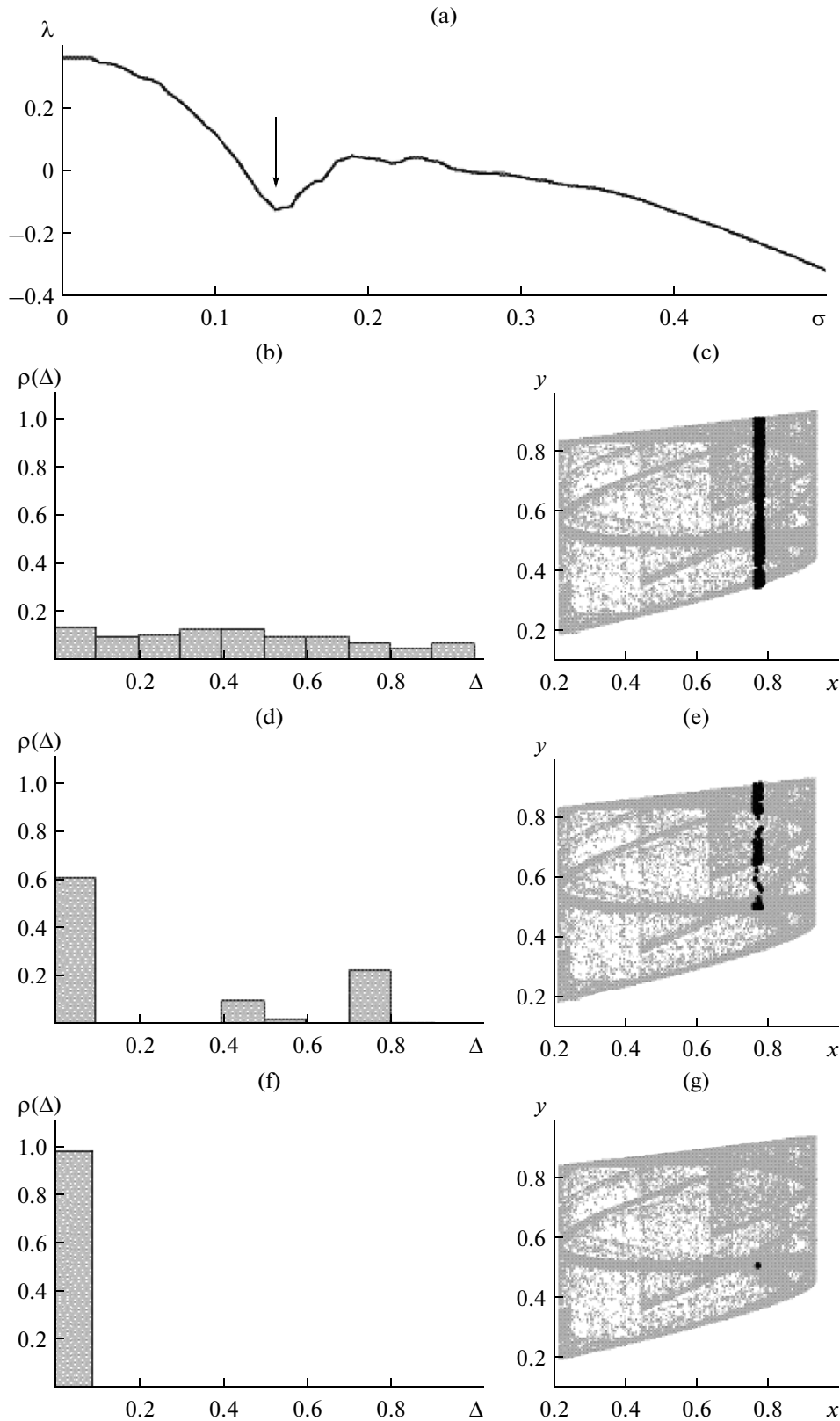


Fig. 4. (a) Plot of conditional Lyapunov exponent λ vs. coupling parameter σ (the arrow shows $\sigma = 0.14$); (b), (d), and (f) histograms of normalized difference Δ ; and (c), (e), and (g) planes (x, y) for two unidirectionally coupled logistic mappings (29) in the generalized synchronization regime for prehistory lengths $K =$ (b) and (c) 0, (d) and (e) 10, and (f) and (g) 28 and (c), (e), and (g) the states of interacting systems that satisfy condition (26).

ferences. For example, the distribution at $K = 10$ exhibits several developed peaks that emerge due to the nonuniformity of chaotic attractor (Fig. 4d). However, in this case, points y_j in the phase space of the response system are still distributed in a wide range of variable y (Fig. 4e). Figures 4f and 4g present similar distributions for the optimal prehistory length $K = 28$. In this case, the distribution of normalized differences represents a δ function (Fig. 4f). States of the system (x_j, y_j) that satisfy condition (22) are concentrated in the small neighborhood of reference point (x_N, y_N) (Fig. 4g). The fractal character vanishes, and the relation of the states of the drive and response systems becomes smooth as in the case of strong synchronization.

In general, the prehistory must be taken into account in the correct analysis of the state vectors of two unidirectionally coupled logistic mappings, so that the results become similar to those obtained for the system with continuous time.

In the *second example*, we consider two mutually coupled Henon mappings

$$\begin{aligned} x_{n+1}^1 &= f(x_n^1, x_n^2, a_x) + \sigma(f(y_n^1, y_n^2, a_y) - f(x_n^1, x_n^2, a_x)), \\ x_{n+1}^2 &= bx_n^1, \\ y_{n+1}^1 &= f(y_n^1, y_n^2, a_y) + \sigma(f(x_n^1, x_n^2, a_x) - f(y_n^1, y_n^2, a_y)), \\ y_{n+1}^2 &= by_n^1, \end{aligned} \quad (30)$$

where $\bar{x} = (x^1, x^2)$ [$\bar{y} = (y^1, y^2)$] are the state vectors of the first [second] system; $f(x_1, x_2, a) = ax_1(1 - x_1) + x_2$ is the nonlinear function; $a_x = 3.16779$, $a_y = 2.9$, and $b = 0.3$ are the control parameters; and σ is the coupling parameter [10, 21]. For these control parameters, the generalized synchronization that is determined using the moment at which one of two Lyapunov exponents becomes negative [11, 12] emerges at $\sigma \approx 0.035$.

Then, we fix coupling parameter $\sigma = 0.2$ and perform the study that is similar to the above study of system (30). The weak GCS is observed in the system under study at $\sigma = 2$. As in the previous case, we characterize the closeness of vectors \bar{y}_j and \bar{z}_j using normalized differences (24) and the analysis of the positions of vectors \bar{y}_j and \bar{z}_j on the (y^1, y^2) plane. Figure 5 shows the distributions of normalized differences Δ_j and vectors \bar{y}_j and \bar{z}_j for two different scenarios. In the first scenario (Figs. 5a and 5b), we employ all of nearest neighbors (the prehistory is disregarded and $K = 0$). In the second scenario (Figs. 5c and 5d), we take into account the prehistory with length $K = 40$. In both cases, we use $\varepsilon = 0.01$ in expression (26). It is seen that normalized difference Δ_j in the first scenario is almost uniformly distributed over unit interval (as in the case of the above logistic mappings) and vectors \bar{y}_j and \bar{z}_j significantly differ from each other, which indi-

cates the absence of a smooth functional relation of the states of interacting Henon mappings. However, in the second scenario with the prehistory taken into account, the distribution of differences Δ_j represents a δ function and calculated vectors \bar{z}_j are in good agreement with vectors of the second system \bar{y}_j . This circumstance indicates the correctness of the theoretical analysis of Section 2.

Thus we conclude that the prehistory of mappings must be taken into account in the analysis of the relation of state vectors in the interrelated 2D mappings.

4. STRONG AND WEAK GENERALIZED SYNCHRONIZATION

Finally, we discuss the commonly accepted concept of strong and weak GCS (see, for example, [5] and Section 3.2). As was mentioned in the Introduction, the conventional approach involves the classification of the generalized synchronization (strong or weak) based on the properties of the functional state that is established between the interacting systems. At a relatively low coupling strength of the systems, functional relation \mathbf{F} is fractal and, hence, the weak synchronization takes place.⁴ If the coupling strength is relatively high, the functional relation is smooth and we obtain the total synchronization or synchronization with delay, which are classified as the strong modifications of the generalized synchronization. The above statements [14] are based on the calculation of the correlation dimension (and the remaining characteristics) of attractors in phase space $D \oplus R$ (D and R are phase spaces of the drive and response oscillators, respectively).⁵

Indeed, the analysis of the attractor of two coupled logistic mappings in space $D \oplus R$ (see, for example, Fig. 4c) shows the fractal properties. At the same time, the observed fractality is an artifact that is related to the assumption on the existence of simple functional relation (4) of the states of interacting systems with disregard of the prehistory. To take into account the prehistory in phase space $D \oplus R$, we must consider only vectors \bar{y}_j that satisfy condition (26) (condition (25) for flow systems) (Fig. 4g). It is seen that all of states (x_j, y_j) are concentrated in a small neighborhood of reference point (x_N, y_N) , the fractality vanishes, and relation \mathbf{F} of the states of interacting systems is smooth. A similar conclusion can be drawn for not only logistic mappings (29) but also alternative flow systems and discrete mappings.

⁴ As was mentioned, this statement is valid for unidirectionally coupled flow systems and unidirectional invertible mappings.

⁵ It is commonly accepted that the dimension of strange attractor for fractal mapping \mathbf{F} in total phase space $D \oplus R$ is greater than the dimension of attractor of the drive system in space D whereas the dimensions must coincide for smooth mapping \mathbf{F} .

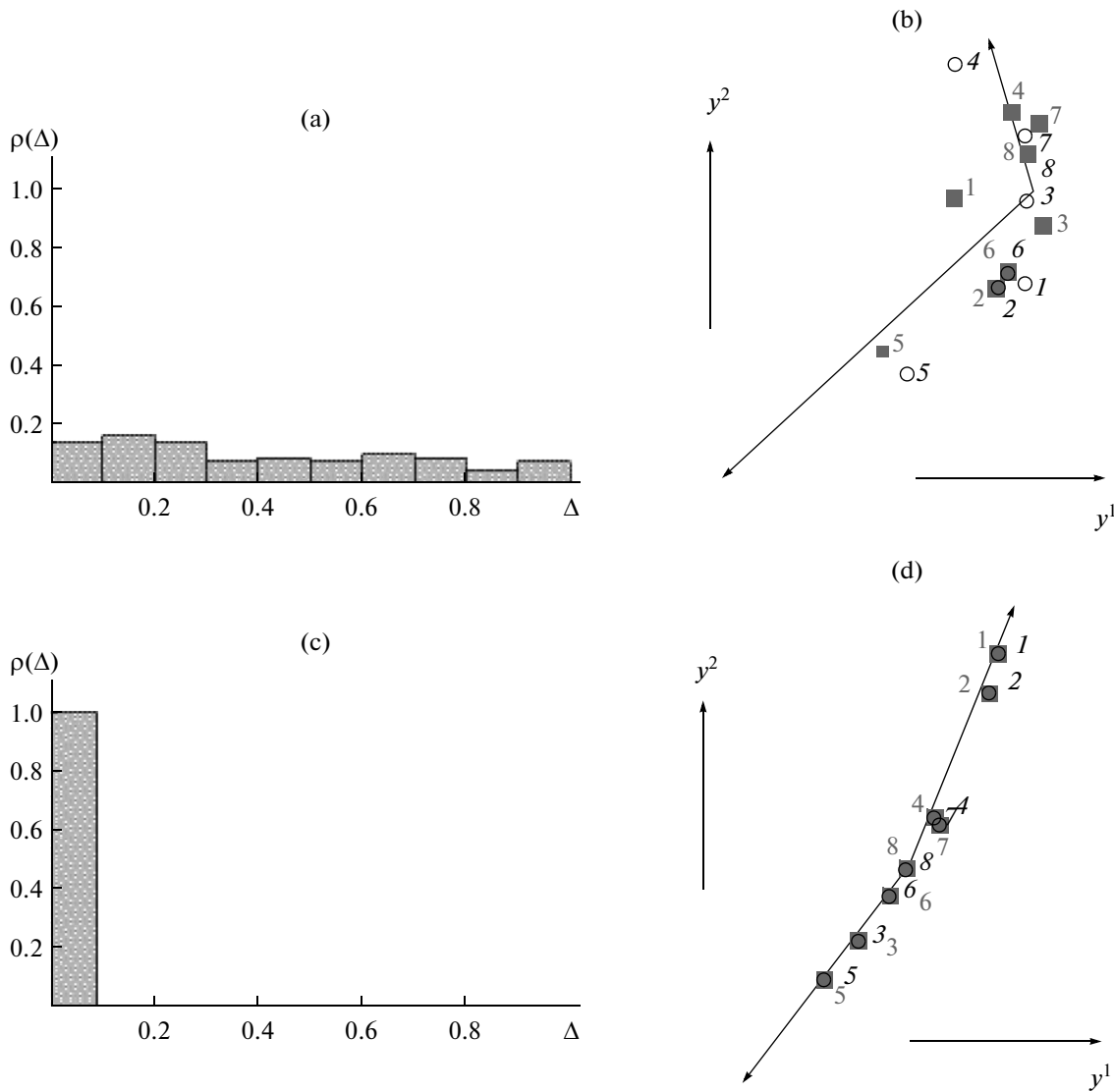


Fig. 5. (a) and (c) Histograms of normalized difference Δ and (b) and (d) vectors (closed squares 1–8) \bar{y}_j and (open circles 1–8) \bar{z}_j for the second Henon mapping (30) at $\sigma = 0.2$ and prehistory lengths $K =$ (a) and (b) 0, (c) and (d) 40.

Thus, we must employ the specified concept of the strong and weak GCS. The specification lies in the fact that state $\bar{y}(t)$ [\bar{y}_n] of the second system depends on both state of first system $\bar{x}(t)$ [\bar{x}_n] at the same time moment and the prehistory of the state with duration τ [K]. In other words, relationships (12) [(13)] are satisfied for the states of interacting systems in the weak-synchronization regime. An increase in the coupling parameter leads to a decrease in the prehistory length, which reaches zero at a certain coupling parameter, so that the total synchronization is established. In this case, the states of interacting systems are interrelated with functional relations (3) [(4)] and the regime under study corresponds to the strong generalized synchronization.

Hence, the classification of the GCS (strong and weak) is valid. However, the difference of the regimes is not determined by the type of relation \mathbf{F} (smooth or fractal) of the states of interacting systems, since it is smooth in both cases. In the strong-synchronization regime functional relations (3) [(4)] are satisfied for the states of interacting systems whereas the prehistory must be taken into account in the weak-synchronization regime.

CONCLUSIONS

We have studied the GCS in the unidirectionally mutually coupled flow systems and discrete mappings. It is demonstrated that the existing GCS concept must be corrected and specified, since the states of the sys-

tems are generally interrelated as a functional. A method for the analysis of the generalized synchronization in such systems is proposed. The results are illustrated using examples of unidirectionally coupled Rössler systems, mutually coupled oscillators based on tunnel diode, unidirectionally coupled logistic mappings, and mutually coupled Henon mappings.

The results show that the classification of the generalized synchronization (weak and strong) needs to be reconsidered and specified: the states of interacting systems in the strong-synchronization regime satisfy a functional relation whereas the prehistory must be taken into account in the analysis of the weak synchronization. For both strong and weak synchronization, a smooth relation is satisfied for states of interacting systems and the fractality vanishes when the prehistory is correctly taken into account.

ACKNOWLEDGMENTS

This work was supported by the Ministry of Education and Science of the Russian Federation (project no. 1776 for state research, order nos. SGTU-141 and SGTU-146) and the Russian Foundation for Basic Research (project no. 12-02-00221a).

REFERENCES

1. L. Glass, *Nature* **410** (6825), 277 (2001).
2. S. Boccaletti, J. Kurths, G. V. Osipov, et al., *Phys. Reports* **366** (1–2), 1 (2002).
3. A. A. Koronovskii, O. I. Moskalenko, and A. E. Khramov, *Usp. Fiz. Nauk* **179**, 1281 (2009).
4. N. F. Rulkov, M. M. Sushchik, L. S. Tsimring, and H. D. I. Abarbanel, *Phys. Rev. E* **51**, 980 (1995).
5. K. Pyragas, *Phys. Rev. E* **54**, R4508 (1996).
6. H. D. I. Abarbanel, N. F. Rulkov, and M. M. Sushchik, *Phys. Rev. E* **53**, 4528 (1996).
7. L. Kocarev and U. Parlitz, *Phys. Rev. Lett.* **76**, 1816 (1996).
8. A. A. Koronovskii, A. E. Hramov, and A. E. Khramova, *JETP Lett.* **82**, 160 (2005).
9. U. Parlitz, L. Junge, W. Lauterborn, and L. Kocarev, *Phys. Rev. E* **54**, 2115 (1996).
10. K. Pyragas, *Phys. Rev. E* **56**, 5183 (1997).
11. O. I. Moskalenko, A. A. Koronovskii, A. E. Hramov, and S. A. Shurygina, in *Proc. 18th IEEE Workshop on Nonlinear Dynamics of Electronic Systems (NDES-2010), Dresden, May 26–28, 2010* (Univ. Technol., Dresden, 2010), p. 70.
12. A. A. Koronovskii, O. I. Moskalenko, V. A. Maksimenko, and A. E. Khramov, *Tech. Phys. Lett.* **37**, 610 (2011).
13. A. A. Koronovskii and A. E. Khramov, *Tech. Phys. Lett.* **30**, 998 (2004).
14. A. E. Hramov and A. A. Koronovskii, *Phys. D (Amsterdam)* **206** (3–4), 252 (2005).
15. A. E. Hramov and A. A. Koronovskii, *Phys. Rev. E* **71**, 067201 (2005).
16. A. A. Koronovskii, O. I. Moskalenko, and A. E. Khramov, *Tech. Phys.* **51**, 143 (2006).
17. A. E. Hramov, A. A. Koronovskii, and O. I. Moskalenko, *Europhys. Lett.* **72**, 901 (2005).
18. M. G. Rosenblum, A. S. Pikovsky, and J. Kurths, *IEEE Trans. Circuits Syst., I: Fundam. Theory Appl.* **44**, 874 (1997).
19. A. A. Koronovskii, M. K. Kurovskaya, O. I. Moskalenko, and A. E. Khramov, *Tech. Phys.* **52**, 19 (2007).
20. A. E. Hramov, A. A. Koronovskii, and O. I. Moskalenko, *Phys. Lett. A* **354**, 423 (2006).
21. K. Pyragas, *Nonlinear Analysis: Modelling and Control*, No. 3, 101 (1998).

Translated by A. Chikishev